

Enabling *ab initio* configurational sampling of multicomponent solids with long-range interactions using neural network potentials and active learning

Shusuke Kasamatsu,^{1,*} Yuichi Motoyama,² Kazuyoshi Yoshimi,²
Ushio Matsumoto,^{3,4} Akihide Kuwabara,³ and Takafumi Ogawa^{3,†}

¹*Academic Assembly (Faculty of Science), Yamagata University,
1-4-12 Kojirakawa, Yamagata-shi, Yamagata 990-8560 JAPAN*

²*The Institute for Solid State Physics, the University of Tokyo,
5-1-5 Kashiwanoha, Kashiwa-shi, Chiba, 277-8581, JAPAN.*

³*Nanostructures Research Laboratory, Japan Fine Ceramics Center,
2-4-1 Mutsuno, Atsuta-ku, Nagoya 456-8587 JAPAN.*

⁴*Department of Materials Science and Engineering, Kyoto University,
Yoshida-Honmachi, Sakyo-ku, Kyoto 606-8501, JAPAN.*

We propose a scheme for *ab initio* configurational sampling in multicomponent crystalline solids using Behler-Parinello type neural network potentials (NNPs) in an unconventional way: the NNPs are trained to predict the energies of relaxed structures from the perfect lattice with configurational disorder instead of the usual way of training to predict energies as functions of continuous atom coordinates. Training set bias is avoided through an active learning scheme. This idea is demonstrated on the calculation of the temperature dependence of the degree of A/B site inversion in MgAl_2O_4 , which is a multivalent system requiring careful handling of long-range interactions. The present scheme may serve as an alternative to cluster expansion for ‘difficult’ systems, e.g., complex bulk or interface systems with many components and sublattices that are relevant to many technological applications today.

INTRODUCTION

Configurational order/disorder determines many properties of functional materials including mechanical strength, catalytic activity, ion/electron/phonon conductivity, and so on. Configurational disorder can be predicted using Monte Carlo (MC) methods based on statistical mechanics, but MC methods usually require a huge number of energy evaluations. Because of this, most works in the past have relied on effective low-cost models that are fitted to density functional theory (DFT) calculations [1–3]. For solid-state systems that can be mapped onto a lattice, the cluster expansion method [4–10] is often considered the *de facto* standard for obtaining such effective models. This method describes configuration energies using an expansion based on effective cluster interactions (ECIs) :

$$E(\vec{\sigma}) = \sum_{\alpha} m_{\alpha} V_{\alpha} \Phi_{\alpha}(\vec{\sigma}), \quad (1)$$

where α denotes empty, single, and multi-component clusters, m_{α} is the cluster multiplicity, V_{α} is the ECI, and $\vec{\sigma}$ is the occupation vector. Φ_{α} is the cluster basis function, which for a binary system takes the simple form of

$$\Phi_{\alpha}(\vec{\sigma}) = \prod_{p \in \alpha} \sigma_p, \quad (2)$$

where p are site indices and $\sigma_p \pm 1$ depending on which component occupies site p . Appropriate basis functions for systems with more components can also be generated according to, e.g., Ref. 7.

The ECIs are usually fitted to energies of relaxed structures from small-scale DFT calculations, then used to calculate energies of a much larger supercell in the course of MC sampling calculations. Although this cluster expansion approach has seen much success, especially for metallic alloys, certain limitations and difficulties have also been pointed out over the years. A rather problematic issue is the difficulty in describing complex long-range interactions [11], which becomes important for many technologically relevant systems including many-component oxide systems as well as electrochemical interfaces. Also, the accuracy of the cluster expansion energy prediction is known to degrade when there is significant lattice relaxation [12]. In fact, cluster expansion with constant ECIs is, in a way, a zeroth order approximation and formally cannot provide an exact fitting including relaxation effects [8]. Another difficulty is in choosing the finite number of clusters that will give the best predictions. Still another issue is in how to avoid training set bias. These issues are, in fact, highly non-trivial, and developing robust methods for cluster and training set selection is still an area of active research [6, 10, 11, 13, 14]. Also, cluster expansion becomes computationally demanding in a combinatorial way as the number of components and sublattices increases, and this limits the number of clusters that can be included in the expansion [9].

In view of these issues, we as well as some other workers have opted to bypass fitted models and sample directly on DFT energies [15–18]. Using more sophisticated MC schemes that are suited for parallel computation such as Wang-Landau [19] or replica exchange Monte

Carlo (RXMC) [20] sampling, sufficient statistical sampling has been achieved on calculation models with up to a few hundred atoms. However, some of these works required weeks of calculations on up to 100 supercomputer nodes, and much acceleration is necessary if this type of approach is to be used in a more widespread manner on a variety of materials systems. Towards this end, we consider, in this work, the so-called “active learning” approach, which has been developed to accelerate first-principles molecular dynamics simulations or MC calculations [21–28]. The basic idea is to use machine-learning potentials (MLPs) that have been fitted to DFT results to accelerate the calculations. Since MLPs are usually good at interpolating but not at extrapolating, a relearning is performed when the system wanders into a previously unlearned region of structure space, then the simulation is restarted with the newly tuned potential. Here, we apply this idea to the lattice configuration problem.

Many forms of MLPs have been proposed in the literature; in this work, we employ the high-dimensional neural network potential (NNP) scheme proposed by Behler and Parinello [29–31]. This scheme assumes that the total energy can be decomposed into atomic energies determined by the environment around each atom, and uses neural networks to fit these atomic energies. To characterize atomic environments, we employ the Chebyshev polynomial-based fingerprint proposed by Artrith *et al.* [32]; the effectiveness of this fingerprint function has been demonstrated especially for multicomponent systems. Atomic Energy NETWORK (ænet) code [32, 33] is employed for the NNP training.

A distinguishing point of this work compared to the literature on Behler-Parinello NNPs is that we train the NNP model to predict the total energies of relaxed structures from unrelaxed ideal lattice structures with configurational disorder. This is quite different from the usual approach of learning the total energies as a function of continuous atom coordinates (the only exception we are aware of is Ref. 34, which used the NNP scheme to describe the relaxation energy when a single Cu interstitial is dissolved in amorphous Ta₂O₅). In a sense, this is a “lazy” alternative to the cluster expansion method without the need to explicitly consider optimized bases, i.e., clusters; there is also no need to perform any explicit basis reduction based on lattice symmetry. Thus, it should be much easier to apply to multicomponent and multi-sublattice systems. We can also use the same fingerprint functions for bulk, surface, and interface systems, while cluster expansion requires more clusters for non-bulk systems [35]. Another merit is that the nonlinearity of the NNP model can lead to better convergence in practice compared to linear models (such as the cluster expansion) [32]. Still, the choice of input structures in the training is just as problematic as other approaches. In fact, we demonstrate a rather spectacular failure when training only on randomly generated configurations, and

then show how well the active learning approach can solve this issue.

As a side note, we point out that the NNP can be directly trained to predict the energy as a function of the configuration vector $\vec{\sigma}$, as was done in Ref. 36. However, the transferability of the NNP to larger supercells in such a scheme is nontrivial, and thus we advocate the use of atom-centric fingerprint functions. It is also possible to perform nonlinear cluster expansion, i.e., fitting the total energy as a function of cluster correlations using a neural network [37]. Yet another successful model is the low rank potential, which expresses the interatomic potential as a low rank decomposition of a tensor whose indices specify the local atomic environment [26, 38]. We do not claim that the approach presented in this work is an overall better method, as it is difficult to compare overall performance including calculation speed, accuracy, and ease-of-use on equal footing. However, as noted above, cluster selection or explicit mapping to a tensor-like expression required in other schemes can be intractable with increasing complexity of the system. Thus, we believe that the current approach will enable configurational sampling in complex bulk or interface systems with many components and sublattices, i.e., those systems where it is technically difficult to employ previously proposed approaches.

RESULTS AND DISCUSSION

Benchmark system: MgAl₂O₄

We demonstrate the above idea on the calculation of the A/B-site inversion in MgAl₂O₄ spinel. This system is a prototypical multivalent system (i.e., Al³⁺ and Mg²⁺ share lattice sites) where a naive cluster expansion can lead to large qualitative errors due to overfitting in a small calculation cell; augmentation with a screened point charge model (CE-SPCM) was found to be necessary to obtain accurate predictions without considering rather long-range pair clusters in Ref. 11. Also, the feasibility of avoiding cluster expansion fitting and sampling directly on DFT-relaxed energies was demonstrated in combination with RXMC sampling in Ref. 17 with a 48-cation model. Here, we consider a 192-cation model, which is completely beyond the reach of direct DFT sampling for two reasons: (1) because of the longer time required for each DFT calculation, and (2) the *much* larger configurational space that has to be sampled. Regarding (2), the number of degrees of freedom for the 48 cation model is ${}_{48}C_{16} \sim 2 \times 10^{12}$, while that for the 192 cation model is ${}_{192}C_{64} \sim 7 \times 10^{51}$. This explosion in the configuration space should attest to the curse of dimensionality that we are fighting against, although there is actually no need to perform calculations on all of these configurations if good sampling schemes (such as RXMC) are

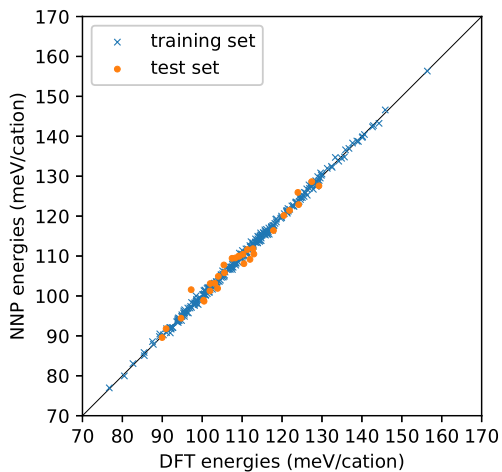


FIG. 1. The results of NNP training on 300 randomly chosen configurations. The zero reference for the energy is taken to be the DFT energy for the ordered spinel configuration.

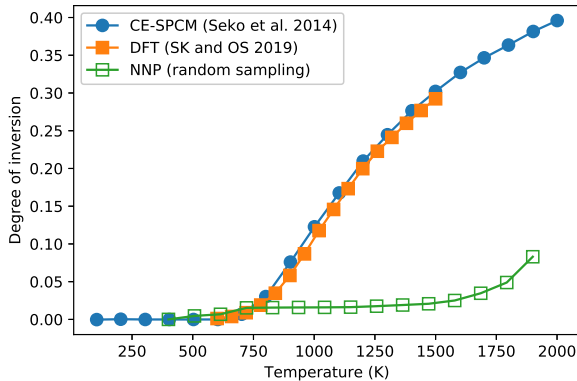


FIG. 2. The degree of inversion calculated in the 192-cation cell using NNPs trained on randomly sampled configurations (green open squares). The results are also compared to previous theoretical works using cluster expansion augmented with a screened point charge model (CE-SPCM; 48 000 cations; orange squares) [11], and that using direct sampling on DFT energies (48 cations; blue circles) [17].

available.

Failure of random sampling

We start the active learning process with 300 randomly chosen configurations. DFT relaxation and energy calculations are performed on these configurations, then an NNP set is trained to predict relaxed energies from the input configurations. The oxygen sublattice is neglected in the training process since the input structures all have identical oxygen coordinates and do not provide any useful information for the prediction. We used 90% of input structures for training and 10% for testing. The results

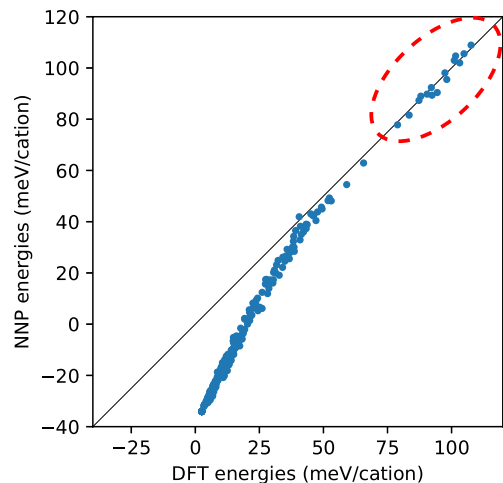


FIG. 3. Comparison of NNP predictions and DFT results for 300 configurations sampled from the RXMC runs. The NNP was trained on random configurations as shown in Fig. 1. The red dashed circle indicates the energy region that was included in the training set.

of the fitting are shown in Fig. 1, with mean absolute error (MAE) of 0.4 meV/cation and root mean square error (RMSE) of 0.5 meV/cation for the training set, and MAE of 1.3 meV/cation and RMSE of 1.6 meV/cation for the test set. In other words, the fitting is working very well considering the fact that these values are already very close to the accuracy limitation of the DFT calculations that the NNPs are being trained to mimic. However, a serious problem becomes evident when we use the trained NNP in the RXMC sampling of the degree of A/B-site inversion (DOI) as shown in Fig. 2. The DOI, which is calculated as the ratio of Al ions on Mg sites, is severely underestimated in the entire temperature range being considered (up to 1900 K) compared to previous theoretical works (it should be noted that previous theoretical works are in fairly good agreement with available experimental data above 1000 K; deviation from experiment is seen at lower temperatures, where cations are not mobile enough to reach equilibrium under most experimental conditions [11, 17]). To understand the source of this error, we sampled 300 structures from the first 6400 RXMC steps (20 structures from each temperature), performed DFT relaxations on them, and compared the NNP prediction and DFT results as shown in Fig. 3. The NNP is found to systematically underestimate the energy of the lower energy configurations, i.e., those with less disorder. This, in turn, results in an overestimation of energy differences, making it less likely to jump to disordered configurations during the MC sampling. Such inaccuracy, in hindsight, is quite reasonable, since the NNP was trained on randomly generated structures, and the training set did not include the more ordered structures with lower energies. The importance of removing such training set bias has already been pointed out in the cluster expansion liter-

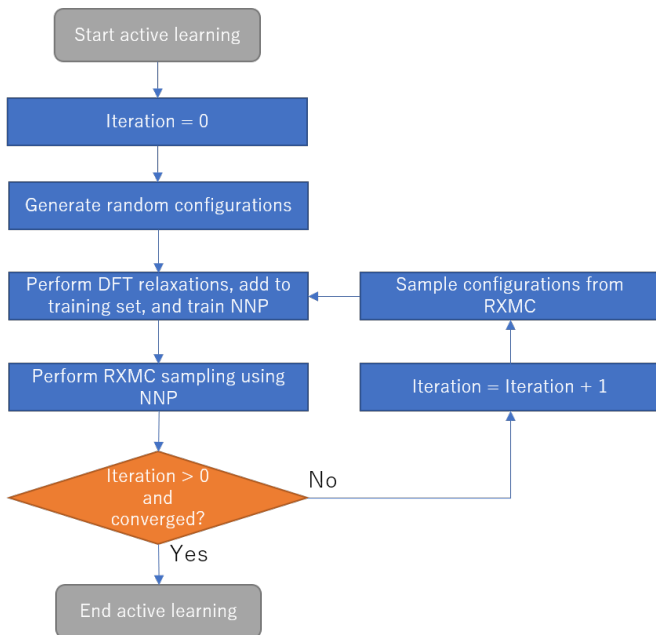


FIG. 4. A flowchart of our configurational sampling scheme using active learning.

ature. A suggested solution was to perform a grouping of input structures based on correlation functions (which roughly corresponds to the degree of disorder), and to perform cross validation on each group during the fitting process [13]. We take an alternate approach, i.e., active learning; we simply add the structures that appear during the RXMC sampling to the training set, retrain the NNPs, and run RXMC sampling again (Fig. 4). This process was repeated 4 times to obtain a converged result.

Active learning

Figure 5 shows the NNP prediction in the first and fourth active learning iterations compared to DFT results. Again, 300 configurations were sampled from the corresponding RXMC runs and DFT relaxations were performed on those samples. The accuracy of the NNP is already quite good after the first active learning step, where the maximum error is about 0.6 eV (3 meV/cation). The maximum error reduces to about half of that value after the fourth iteration. The DOI results are shown in Fig. 6. The DOI turns out to be well converged already at the first iteration. The results are also quite similar to previous works, although the current work estimates the DOI above 600 K to be slightly larger than previous works. It is difficult to judge whether the current work is more accurate than the CE-SPCM approach of Ref. 11; the learning is performed in a much larger supercell here (192 cation model vs. 18–30 cation

model in Ref. 11), but the MC calculations are performed in a much smaller cell (192 vs. 48 000). Unfortunately, NNP evaluation is not as fast as cluster expansion at this point, and it is not fast enough to enable sufficient sampling on a 48 000-cation model. Still, on the Xeon E5-2680v3 CPU, the NNP prediction using 1 CPU core is a few hundred times faster than DFT relaxation using 216 cores. The speedup will be much more significant on more difficult to relax systems; the MgAl_2O_4 system relaxes exceptionally easily within a little more than 10 ionic steps, but other systems such as doped perovskites with oxygen vacancies [18] can take more than 100 ionic steps to obtain a relaxed structure. We also note that the number of necessary DFT calculations turned out to be orders of magnitude smaller than the number of NNP evaluations necessary for converging the DOI; a single iteration of active learning required 600 DFT calculations in total (300 random samples plus 300 samples from the first RXMC run), while $\sim 7\,200\,000$ NNP evaluations (= 480 000 MC steps/replica \times 15 replicas) were necessary to obtain a converged DOI vs. temperature. The 600 DFT calculations can be completed within a few hours on a modern supercomputer system since the calculations can be performed completely in parallel. The RXMC calculations took roughly one day using 15 CPU cores, which would fit in one node of a modern workstation.

An additional point that we were interested in is how well the NNP trained on a smaller supercell can describe configuration statistics in larger supercells. In the case of cluster expansion, overfitting to a small unit cell can occur when choosing the best clusters to minimize the cross validation scores [11]. To examine this, we trained the NNP using active learning on the conventional MgAl_2O_4 unit cell with 24 cations, then used this to sample the $2 \times 2 \times 2$ supercell with 192 cations. The results are in fairly good agreement with active learning results on the 192-cation cell as well as previous works (Fig. 6), suggesting that the Chebychev fingerprint is doing a fairly good job of balancing short, middle, and long-range interactions, even when trained in a relatively small unit cell.

Finally, we note that the accuracy of the NNP demonstrated here for predicting relaxed energies is probably the best case scenario, since the spinel lattice turns out to be quite rigid. For more difficult cases with significant relaxation, it may be advisable to perform the active learning scheme for a few iterations, then use the final NNP in nested Monte Carlo [39–42] or upsampling schemes [43], where MC or MD steps are carried out with low cost potentials then augmented with DFT calculations at preset intervals. These schemes are guaranteed to converge to the same result as sampling based only on DFT energies, and the speedup will depend on the quality of the low cost potential. We plan on implementing and testing such schemes in the near future.

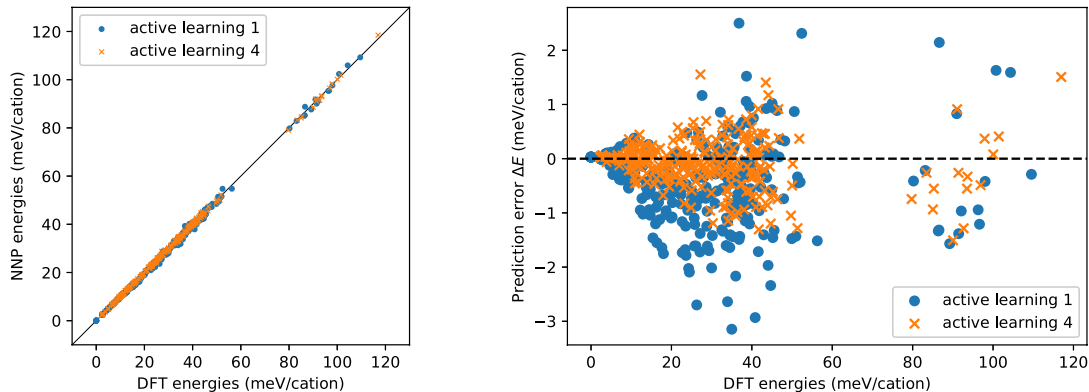


FIG. 5. Comparison of NNP predictions and DFT results after the first and fourth active learning iterations.

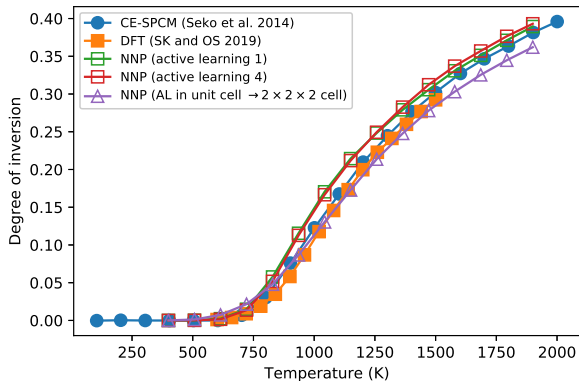


FIG. 6. The degree of inversion calculated after the first (green open squares) and fourth (red open squares) active learning iterations, and that calculated using NNP active-learned in the conventional unit cell (purple triangles).

METHODS

DFT calculations

The DFT calculations were performed using VASP code [44, 45]. We employed the projector augmented wave method [46] to describe electron-ion interactions. A plane wave basis set with an energy cutoff of 300 eV was used to expand the wave functions. The Brillouin zone was sampled only at the Γ point. The GGA-PBE functional [47] was used to approximate the exchange-correlation energy.

NNP training and evaluation

The NNP training and subsequent evaluation were performed using $\text{\ae}net$ code [33]. We used the fingerprint-

ing scheme by Artrith *et al.* [32], where the radial and angular distribution functions (RDF and ADF) with an appropriately chosen cutoff are expanded by an orthogonal basis set based on Chebyshev polynomials, and the expansion coefficients are fed in to the neural network as the input descriptors. A key point in their scheme is that the structural and compositional descriptors are given separately; the structural descriptor is given by the usual RDF and ADF, and the compositional descriptor is also given by RDF and ADF but with atomic contributions weighted differently for each chemical species. In this work, we expand the RDF with a cutoff of 8.0 Å and expansion order 16 and the ADF with a cutoff of 6.5 Å and expansion order 4. The employed neural network thus has an input layer with 44 nodes [48], and we chose to use 2 hidden layers with 15 nodes each and the tanh activation. The training epochs were monitored and terminated when the test set error began to increase.

RXMC sampling

The replica exchange Monte Carlo (RXMC) method combined directly with NNP evaluation using $\text{\ae}net$ was implemented in ab-Initio Configuration Sampling Toolkit (abICS) <https://github.com/issp-center-dev/abICS>. The detailed theory behind RXMC is given in Ref. 20. Our previous works [17, 18] may also be helpful for understanding the basic concept. In this work, 15 replicas of the system were sampled in parallel with temperatures ranging from 400 K to 1900 K, and temperature exchange was attempted every 4 steps to speed up the global sampling. Samples for DFT calculations were drawn from the first 6 400 RXMC steps in the first active learning iteration. In subsequent iterations, the samples were drawn from the first 16 000 steps. For the DOI calculations, 80 000 steps were used for

equilibration and DOI from 400 000 steps were averaged to obtain the temperature dependence. We note, in passing, that the RXMC simulations were initialized with random configurations, and yet they still found the single ground state ordered spinel configuration out of $\sim 10^{51}$ possible configurations. This attests to the effectiveness of modern sampling methods in battling the curse of dimensionality.

ACKNOWLEDGEMENTS

The software used in this work (abICS) was developed in part by “Project for advancement of software usability in materials science” by the Institute for Solid State Physics, the University of Tokyo, and the calculations were performed on the joint-use supercomputer system at the same Institute. This research was supported by “Program for Promoting Research on the Supercomputer Fugaku” (Fugaku Battery & Fuel Cell Project), and by CREST, Japan Science and Technology Agency Grant Number JPMJCR18J3. S. K. acknowledges funding from Japan Society for the Promotion of Science (JSPS) KAKENHI Grant Number 20H05284 (Grant-in-Aid for Scientific Research on Innovative Areas “Interface IONICS”) and 19K15287 (Grant-in-Aid for Young Scientists). T. O. is funded by JSPS KAKENHI Grant Number 19H05792 (Grant-in-Aid for Scientific Research on Innovative Areas “Crystal Defect Core”).

AUTHOR CONTRIBUTIONS

S. K. and T. O. designed the research. U. M. performed preliminary NNP fitting calculations to assess the feasibility of the approach. S. K., K. Y., and Y. M. jointly coded the abICS software. S. K. performed all of the calculations and analyses presented in this paper. All authors contributed to the discussion and steering of the research direction and jointly wrote the paper.

* E-mail: kasamatsu@sci.kj.yamagata-u.ac.jp

† E-mail: t_ogawa@jfcc.or.jp

- [1] Jürgen Hafner, Christopher Wolverton, and Gerbrand Ceder, “Toward Computational Materials Design : The Impact of Density Functional,” *MRS Bull.* **31**, 659–668 (2006).
- [2] Gerbrand Ceder, “Opportunities and challenges for first-principles materials design and applications to Li battery materials,” *MRS Bull.* **35**, 693–701 (2010).
- [3] Jrg Neugebauer and Tilmann Hickel, “Density functional theory in materials science,” *WIREs Comput. Mol. Sci.* **3**, 438–448 (2013).
- [4] J. M. Sanchez, F. Ducastelle, and D. Gratias, “Generalized cluster description of multicomponent systems,” *Physica A* **128A**, 334–350 (1984).
- [5] A. van de Walle, M. Asta, and G. Ceder, “The alloy theoretic automated toolkit: A user guide,” *Calphad* **26**, 539 – 553 (2002).
- [6] Atsuto Seko, Yukinori Koyama, and Isao Tanaka, “Cluster expansion method for multicomponent systems based on optimal selection of structures for density-functional theory calculations,” *Phys. Rev. B* **80**, 165122 (2009).
- [7] J. M. Sanchez, “Cluster expansion and the configurational theory of alloys,” *Phys. Rev. B* **81**, 224202 (2010).
- [8] J. M. Sanchez, “Foundations and Practical Implementations of the Cluster Expansion,” *J. Phase Equilib. Diffus.* **38**, 238–251 (2017).
- [9] Qu Wu, Bing He, Tao Song, Jian Gao, and Siqi Shi, “Cluster expansion method and its application in computational materials science,” *Comput. Mater. Sci.* **125**, 243–254 (2016).
- [10] Jin Hyun Chang, David Kleiven, Marko Melander, Jaakko Akola, Juan Maria Garcia-Lastra, and Tejs Vegge, “CLEASE: a versatile and user-friendly implementation of cluster expansion method,” *J. Phys.: Condens. Matter* **31**, 325901 (2019).
- [11] Atsuto Seko and Isao Tanaka, “Cluster expansion of multicomponent ionic systems with controlled accuracy: importance of long-range interactions in heterovalent ionic systems,” *J. Phys.: Condens. Matter* **26**, 115403 (2014).
- [12] Andrew H. Nguyen, Conrad W. Rosenbrock, C. Shane Reese, and Gus L.W. Hart, “Robustness of the cluster expansion: Assessing the roles of relaxation and numerical error,” *Phys. Rev. B* **96**, 014107 (2017).
- [13] Atsuto Seko and Isao Tanaka, “Grouping of structures for cluster expansion of multicomponent systems with controlled accuracy,” *Phys. Rev. B* **83**, 224111 (2011).
- [14] Zhidong Leong and Teck Leong Tan, “Robust cluster expansion of multicomponent systems using structured sparsity,” *Phys. Rev. B* **100**, 134108 (2019).
- [15] S. N. Khan and Markus Eisenbach, “Density-functional Monte-Carlo simulation of CuZn order-disorder transition,” *Phys. Rev. B* **93**, 024203 (2016).
- [16] Robert B Wexler, Tian Qiu, and Andrew M Rappe, “Automatic Prediction of Surface Phase Diagrams Using Ab Initio Grand Canonical Monte Carlo,” *J. Phys. Chem. C* **123**, 2321–2328 (2019).
- [17] Shusuke Kasamatsu and Osamu Sugino, “Direct coupling of first-principles calculations with replica exchange Monte Carlo sampling of ion disorder in solids,” *J. Phys.: Condens. Matter* **31**, 085901 (2019).
- [18] Shusuke Kasamatsu, Osamu Sugino, Takafumi Ogawa, and Akihide Kuwabara, “Dopant arrangements in Y-doped BaZrO₃ under processing conditions and their impact on proton conduction: a large-scale first-principles thermodynamics study,” *J. Mater. Chem. A* **8**, 12674–12686 (2020).
- [19] Fugao Wang and D. P. Landau, “Efficient, multiple-range random walk algorithm to calculate the density of states,” *Phys. Rev. Lett.* **86**, 2050–2053 (2001).
- [20] Koji Hukushima and Koji Nemoto, “Exchange Monte Carlo Method and Application to Spin Glass Simulations,” *J. Phys. Soc. Jpn.* **65**, 1604–1608 (1996).
- [21] Evgeny V. Podryabinkin and Alexander V. Shapeev, “Active learning of linearly parametrized interatomic potentials,” *Comput. Mater. Sci.* **140**, 171–180 (2017).

- [22] Evgeny V. Podryabinkin, Evgeny V. Tikhonov, Alexander V. Shapeev, and Artem R. Oganov, “Accelerating crystal structure prediction by machine-learning interatomic potentials with active learning,” *Phys. Rev. B* **99**, 064114 (2019).
- [23] Konstantin Gubaev, Evgeny V. Podryabinkin, Gus L.W. Hart, and Alexander V. Shapeev, “Accelerating high-throughput searches for new alloys with active learning of interatomic potentials,” *Comput. Mater. Sci.* **156**, 148–156 (2019).
- [24] Justin S. Smith, Ben Nebgen, Nicholas Lubbers, Olexandr Isayev, and Adrian E. Roitberg, “Less is more: Sampling chemical space with active learning,” *J. Chem. Phys.* **148**, 241733 (2018).
- [25] Linfeng Zhang, De-Ye Lin, Han Wang, Roberto Car, and Weinan E, “Active learning of uniformly accurate interatomic potentials for materials simulation,” *Phys. Rev. Mater.* **3**, 023804 (2019).
- [26] Tatiana Kostiuhenko, Fritz Krmann, Jrg Neugebauer, and Alexander Shapeev, “Impact of lattice relaxations on phase transitions in a high-entropy alloy studied by machine-learning potentials,” *npj Comput. Mater.* **5**, 1–7 (2019).
- [27] Troy D. Loeffler, Tarak K. Patra, Henry Chan, Mathew Cherukara, and Subramanian K. R. S. Sankaranarayanan, “Active Learning the Potential Energy Landscape for Water Clusters from Sparse Training Data,” *J. Phys. Chem. C* **124**, 4907–4916 (2020).
- [28] Jonathan Vandermause, Steven B. Torrisi, Simon Batzner, Yu Xie, Lixin Sun, Alexie M. Kolpak, and Boris Kozinsky, “On-the-fly active learning of interpretable Bayesian force fields for atomistic rare events,” *npj Comput. Mater.* **6**, 20 (2020).
- [29] Jrg Behler and Michele Parrinello, “Generalized Neural-Network Representation of High-Dimensional Potential-Energy Surfaces,” *Phys. Rev. Lett.* **98**, 146401 (2007).
- [30] Jrg Behler, “Atom-centered symmetry functions for constructing high-dimensional neural network potentials,” *J. Chem. Phys.* **134**, 074106 (2011).
- [31] Jrg Behler, “Constructing high-dimensional neural network potentials: A tutorial review,” *Int. J. Quantum Chem.* **115**, 1032–1050 (2015).
- [32] Nongnuch Artrith, Alexander Urban, and Gerbrand Ceder, “Efficient and accurate machine-learning interpolation of atomic energies in compositions with many species,” *Phys. Rev. B* **96**, 014112 (2017).
- [33] Nongnuch Artrith and Alexander Urban, “An implementation of artificial neural-network potentials for atomistic materials simulations: Performance for TiO₂,” *Comput. Mater. Sci.* **114**, 135–150 (2016).
- [34] Wenwen Li, Yasunobu Ando, and Satoshi Watanabe, “Cu Diffusion in Amorphous Ta₂O₅ Studied with a Simplified Neural Network Potential,” *J. Phys. Soc. Jpn.* **86**, 104004 (2017).
- [35] Koretaka Yuge, Atsuto Seko, Akihide Kuwabara, Fumiyasu Oba, and Isao Tanaka, “Ordering and segregation of a Cu₇₅Pt₂₅ (111) surface: A first-principles cluster expansion study,” *Phys. Rev. B* **76**, 045407 (2007).
- [36] Hyunjun Ji and Yousung Jung, “Artificial neural network for the configuration problem in solids,” *J. Chem. Phys.* **146**, 064103 (2017).
- [37] Anirudh Raju Natarajan and Anton Van der Ven, “Machine-learning the configurational energy of multi-component crystalline solids,” *npj Comput. Mater.* **4**, 56 (2018).
- [38] A. Shapeev, “Accurate representation of formation energies of crystalline alloys with many components,” *Comput. Mater. Sci.* **139**, 26–30 (2017).
- [39] Radu Iftimie, Dennis Salahub, Dongqing Wei, and Jeremy Schofield, “Using a classical potential as an efficient importance function for sampling from an ab initio potential,” *J. Chem. Phys.* **113**, 4852 (2000).
- [40] Lev D. Gelb, “Monte Carlo simulations using sampling from an approximate potential,” *J. Chem. Phys.* **118**, 7747–7750 (2003).
- [41] Jeff Leiding and Joshua D. Coe, “Reactive Monte Carlo sampling with an *ab initio* potential,” *J. Chem. Phys.* **144**, 174109 (2016).
- [42] Yuki Nagai, Masahiko Okumura, and Akinori Tanaka, “Self-learning Monte Carlo method with Behler-Parrinello neural networks,” *Phys. Rev. B* **101**, 115111 (2020).
- [43] Xi Zhang, Blazej Grabowski, Tilmann Hickel, and Jrg Neugebauer, “Calculating free energies of point defects from ab initio,” *Comput. Mater. Sci.* **148**, 249–259 (2018).
- [44] G. Kresse and J Furthmüller, “Efficient iterative schemes for ab initio total-energy calculations using a plane-wave basis set,” *Phys. Rev. B* **54**, 11169–11186 (1996).
- [45] G. Kresse and J. Furthmüller, *Comp. Mater. Sci.* **6**, 15 (1996).
- [46] P. E. Blöchl, “Projector augmented-wave method,” *Phys. Rev. B* **50**, 17953–17979 (1994).
- [47] John P Perdew, Kieron Burke, and Matthias Ernzerhof, “Generalized Gradient Approximation Made Simple,” *Phys. Rev. Lett.* **77**, 3865–3868 (1996).
- [48] We have 17 coefficients for RDF and 5 for ADF resulting in 22 descriptors, and this is multiplied by 2 since we have separate RDFs/ADFs for composition and structure.